Experimental and theoretical study of ionization and fragmentation of C_{60} by fast-proton impact

A. Reinköster, U. Werner, N. M. Kabachnik,* and H. O. Lutz
Fakultät für Physik, Universität Bielefeld, D-33615 Bielefeld, Germany
(Received 1 March 2001; published 6 July 2001)

We have studied the ionization and fragmentation of C_{60} in collisions with protons and deuterons at impact energies of 50–300 keV. The time-of-flight spectra of all fragment ions were measured in coincidence with one of the emitted electrons. The cross sections of multiple ionization as well as relative yields of even-mass fullerene-type ions of various charges are deduced from experimental spectra. A theoretical model based on a statistical approach is developed for the explanation of the experimental data. The model describes the $p+C_{60}$ collision as proceeding in three steps: (i) energy deposition by the projectile, (ii) emission of prompt electrons, and (iii) C_2 evaporation and delayed electron emission. The observed distribution of fragment fullerenes indicates that the delayed electron emission is an essential part of the process and that it occurs before the equilibration is achieved.

DOI: 10.1103/PhysRevA.64.023201 PACS number(s): 34.50.Gb, 34.50.Bw

I. INTRODUCTION

During the last decade scattering experiments with fullerenes as collision partners have developed into a vast branch of atomic and molecular collision physics [1,2]. The attraction of fullerenes as an experimental object, namely their availability, highly symmetric shape, stability, absence of isomeric forms, and the fact that they can be easily sublimed into the gas phase, makes them an almost ideal model system for studying the interaction of any agent with a complex molecular system having many degrees of freedom. This is an obvious and straightforward step towards studying complex biomolecular systems. In particular, fullerene collisions with ions and atoms play an important role in understanding such processes as fragmentation, plasmon excitation, energy deposition, and dissipation, etc. A majority of experiments has been done so far at low collision energies [2], i.e., when the main energy-transfer mechanism is the elastic collision of the ion with one or several of the constituent carbon atoms in the fullerene. This is equivalent to nuclear stopping in collisions of ions with solids. In the alternative domain of high-energy collisions the energy is mainly transferred to electronic degrees of freedom (electronic stopping). According to estimations (see, for example, [2]) the elastic scattering and electron excitations give a comparable contribution at collision velocities of about 0.5 a.u. At larger velocities the electronic excitation is the dominant mechanism of energy transfer. In this paper we discuss collisions of fullerenes with high-energy ions at velocities $v>1$ a.u., where the direct energy transfer from projectile to nuclear degrees of freedom is negligible and therefore the only source of energy for the various ionization, excitation, and fragmentation processes is the primary electronic excitation of the fullerene by the projectile ion.

The fast-ion–fullerene collision is a comparatively less studied process. However, a number of experiments were published in which the ionization and fragmentation of C_{60} were studied in collisions with fast protons [3–6], helium ions [3,7,8], lithium, carbon, other light and medium weight ions [3,5,9–11], and highly charged Xe ions [12–14]. A common experimental method used in these investigations is the time-of-flight (TOF) mass spectrometry of charged fragments produced in the collision, often with measuring two or more fragments in coincidence with or without detecting the final charge state of the projectile.

A typical TOF spectrum in collision with a light projectile ion contains peaks that correspond to different mass-to-charge ratios of fragment ions. The peaks fall into three categories: (i) strong and narrow peaks that correspond to multiply ionized ''parent'' fullerenes C_{60}^{q+} with $q=1-5$; each of them is followed by a sequence of (ii) smaller peaks corresponding to even-mass fullerene-type ''daughter'' ions C_{60-2m}^{q+} $(m=1-7)$ which are believed to be mainly formed by successive emission (''evaporation'') of neutral dimers C_2; and finally (iii) the numerous broadened peaks corresponding to mostly singly charged small mass fragments C_n^+ $(n=1-19)$. The latter group is associated with the complete breakdown of the fullerene ''cage,'' a process often referred to as ''multifragmentation.'' It was found that the relative strength of these groups depends drastically on the projectile [3,5] and strongly varies with the collision velocity [7,8]. In particular, the role of multifragmentation increases dramatically with increasing projectile mass and charge. This is intuitively clear since the interaction strength and therefore the energy transfer for highly charged heavy ions is large, leading to a complete disintegration of the fullerene. On the contrary, the fast-proton interaction with C_{60} is comparatively weak, and as shown by experiments [3,4,6], in this case the multifragmentation is almost negligible. Here the main dissipation processes are multiple ionization and evaporation of C_2 neutrals.

In this paper we present the results of an experimental and theoretical study of ionization and fragmentation of C_{60} by fast-proton and -deuteron impact. The velocity range covered by our experiment is from 1.0 to 3.5 a.u. It partly overlaps with the range of the recently published experiments [6] where mainly smaller proton velocities have been used. Our

*On leave from Institute of Nuclear Physics, Moscow State University, Moscow 119899, Russia.

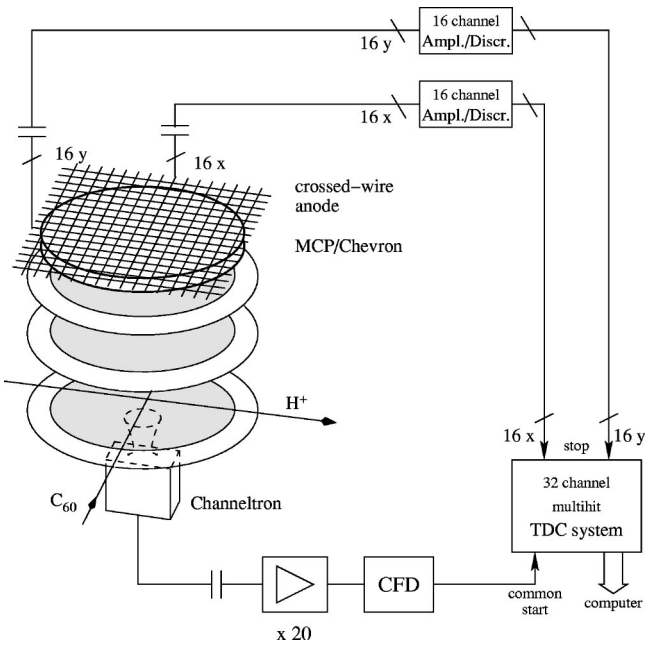

FIG. 1. Experimental setup and coincidence electronics.

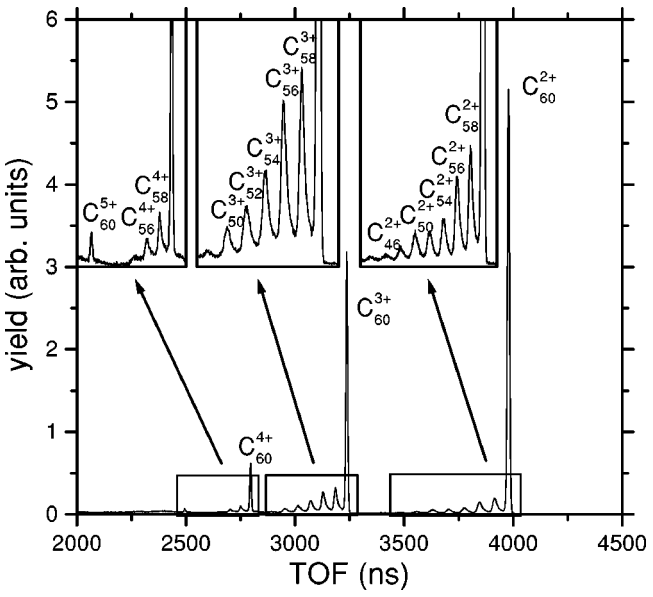

FIG. 2. Part of the time-of-flight spectrum of positive particles produced in 300-keV proton-fullerene collisions. In the insets parts of the spectra are shown in more detail.

new experimental data are more detailed and permit a thorough theoretical analysis. On the high velocity side our experiment overlaps with that by Tsuchida *et al.* [4] who published the data in the velocity range of 2.8–8.9 a.u. Thus, experimental data of a comparable quality are now available for the theoretical analysis in a wide range of proton velocities. In the theoretical part of the paper we suggest a model based on a statistical approach for a description of both the multiple ionization and fragmentation of C_{60} in collisions with protons. A short overview of the theoretical methods previously used for the analysis of fast-ion–fullerene collisions will be given in that part. We shall also present the analysis of the experimental data based on our model. Atomic units are used throughout unless otherwise indicated.

II. EXPERIMENT

A. Experimental setup and data analysis

A more detailed account of the experimental setup is given in Refs. [15–17]. Briefly, a collimated beam of H^+ or D^+ ($v \simeq 1$–3.5 a.u.) from a 350-kV cascade ion accelerator interacts with a C_{60} vapor target (99.95% purity) which is sublimated in an oven at temperatures $\approx 550\,^{\circ}\mathrm{C}$ (Fig. 1). The slow ions and electrons generated in the collision are separated by a weak homogeneous electrical field ($E_s = 330$ V/cm). The C_{60}^{q+} ions and positively charged fragments are accelerated towards a time- and position-sensitive multihit detector[1] at one side of the interaction region; at the other side electrons are detected in a channeltron (CEM). The amplified electron signal is processed by a constant-fraction-discriminator (CFD) and serves as a start signal for the time-of-flight coincidence electronics that mainly consists of a multihit time-to-digital converter (TDC) system. The fragment ions are postaccelerated to an energy of $5.5\ \mathrm{kV}\cdot q$ to increase the efficiency of the microchannel plates (MCP). At these energies the detection efficiency for heavy fullerene ions with $q \geqslant 2$ is practically saturated and therefore independent of the charge state. However, the detection of heavy singly charged C_{60}^+ and C_{60-2m}^+ ions is more problematic. Their detection probability is reduced by two effects. Firstly, the contribution of electron capture to ionization is not negligible in the studied energy range [19]. Due to the lack of a start electron these reactions are not detected, leading to smaller intensities than observed in noncoincident measurements. So far no reliable cross sections of electron capture are available in order to estimate this effect. Secondly, the detection efficiency of the MCP that strongly depends on the velocity of the incident particles does not reach saturation for C_{60-2m}^+ ions. The velocity dependence of this efficiency was studied by Itoh *et al.* [10]. For singly charged ions they reported that the relative detection probability P is described by the empirical relation $P = 1 - \exp(-0.0148E - 0.0218E^2)$, where E is the energy of the fullerene ion in keV. This energy dependence that qualitatively agrees with our observations predicts a value of $P \approx 52\%$ for 5.5-keV C_{60}^+ ions. However, investigations of Schlathölter *et al.* suggest a higher relative efficiency of $\approx 85\%$ [20]. Consequently the detection efficiency of heavy singly charged fullerenes is, in contrast to that of the more highly charged species, a rather uncertain quantity.

Figure 2 shows a typical time-of-flight spectrum observed in collisions of 300-keV H^+ with C_{60}. The most prominent features in this spectrum correspond to the C_{60}^{q+} ions ($q = 1$–5) and to the sequences of even numbered fragment fullerenes C_{60-2m}^{q+}. In the low mass region traces of C_{60} mul-

[1]The multihit detection capability and position resolution are especially useful for the analysis of C_{60} multifragmentation and (binary) fission processes [3,18].

tifragmentation occur. The observed intensities of low mass C_n^+ ions ($n \leqslant 10$) show that multifragmentation amounts to $\sim 5\%$ of the fullerene ions intensity; in collisions with 100-keV H^+ this contribution rises to $\sim 10\%$. Although the main part of C_{60-2m}^{q+} ions are produced by successive evaporation of C_2 neutrals, some contribution comes from another type of process, namely, the superasymmetric fissions $C_{60}^{q+} \rightarrow C_{60-2m}^{(q-1)+} + C_n^+$. These reactions cannot be identified in the simple TOF spectrum, but they can be clearly separated in the measured coincidence spectra [3]. These fission processes gain importance at higher fullerene charge states: for instance the probabilities of C_{60}^{4+} fission and C_2 evaporation from C_{60}^{4+} ions are similar, whereas in the case of C_{60}^{3+} ions the fission probability is small and C_2 evaporation clearly dominates with about 90%. A more detailed analysis of super-asymmetric fission processes will be published elsewhere [18].

From the measured time-of-flight spectra the cross sections of various processes can, in principle, be obtained. However, the determination of absolute cross sections is an experimentally demanding task. In our experiment particularly the C_{60} vapor density is rather uncertain; therefore, reliable values can be obtained only for the relative cross sections. In the paper by Tsuchida *et al.* [4] which partly overlaps with our work, the absolute values of the cross sections have been derived from the yields of C_{60}^{q+} and C_{60-2m}^{q+} ions. These values are based on the C_{60} vapor density published by Abrefah *et al.* [21]. It has to be mentioned that in the literature different values of the C_{60} vapor density have been reported (see, e.g., [19]) and, as a consequence, absolute cross sections are determined with some uncertainties. However, to facilitate a comparison we normalize our data to the cross sections obtained by Tsuchida *et al.* [4] using the measured total yield of triply charged fragment fullerenes $Y^{3+} = \Sigma_{m \geqslant 0} I(C_{60-2m}^{3+})$ at 200 keV. At other energies the derived normalization factor has to be corrected by the actual proton flux N_p and the actual C_{60} target density. The latter was assumed to be constant during the measurements. Unfortunately, the reproducibility of the target density is not very good: the experiment yields a standard deviation of $Y^{3+}(E)/N_p(E)$ of about 40% and other investigations, too, show about 25% errors in the reproduction of the C_{60} density [22]. Cross sections for other fullerene ions $\sigma^{q+}(E)$ are calculated simply by $\sigma^{q+}(E) = \sigma^{3+}(E)[Y^{q+}(E)/Y^{3+}(E)]$.

The relative yield of a fullerenelike fragment C_{60-2m}^{q+} is determined by the intensity ratio

$$r_m^{q+} = I(C_{60-2m}^{q+})/I(C_{60}^{q+}). \tag{1}$$

Finally, to characterize the evaporation behavior and the stability of different C_{60}^{q+} ions we have derived the *relative evaporation fraction* f_e^{q+} [7]

$$f_e^{q+} = \frac{\sum_{m \geqslant 1} I(C_{60-2m}^{q+})}{I(C_{60}^{q+}) + \sum_{m \geqslant 1} I(C_{60-2m}^{q+})}, \tag{2}$$

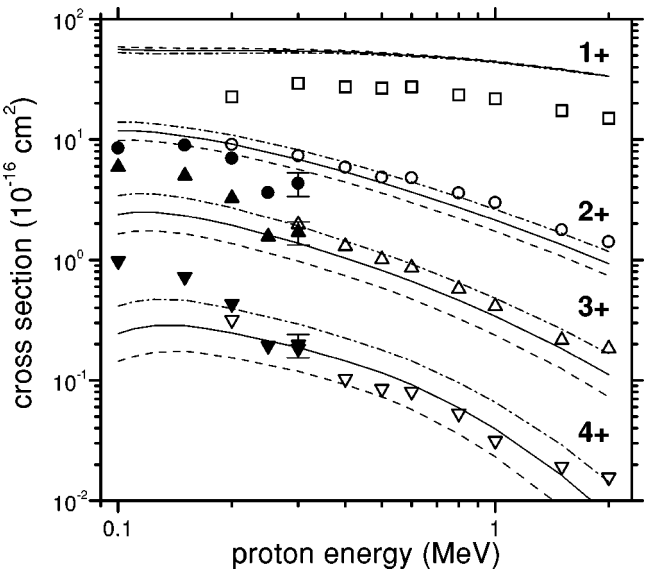

FIG. 3. Cross sections for fullerene ion production σ^{q+} with q from 1 up to 4 for different proton energies. Solid symbols represent our measurements. Cross sections at high proton energies (hollow symbols) are taken from Ref. [4]. Our values are normalized to σ^{3+} at 0.2 MeV. Error bars reflect statistical errors, including those from the poorly reproducible target density. Curves are calculated within the SED model (see Sec. III C) for three different values of the parameter g. Solid curve: $g = 0.007$; dash-dotted curve: $g = 0.01$; dashed curve: $g = 0.005$.

where $I(X)$ denotes the measured intensity of species X. The velocities of the considered fullerene-ions are very similar when they hit the microchannel plates. Therefore, both ratios above are rather insensitive to the mentioned uncertainties in the detection efficiency.

B. Experimental results and comparison with other data

The cross sections σ^{q+} for producing fullerene ions with charge states 1+ up to 4+ by fast-proton impact on C_{60} are presented in Fig. 3. For each charge state q, cross sections σ^{q+} are derived from the sum of the C_{60}^{q+} ion and C_{60-2m}^{q+} fragment-fullerene intensities, detected several μs after the collision. Due to the importance of the (delayed) C_2 evaporation channel, σ^{q+} rather corresponds to the initial charge distribution of C_{60} ions as produced by proton impact. In the high-velocity range cross sections are taken from Ref. [4]. We have not included our data for σ^{1+} in Fig. 3, because of the uncertainty discussed in Sec. II A arising from electron-capture processes in the formation of singly charged fullerene ions and the uncertainty in the detection efficiency. Our experimental cross sections are in acceptable agreement with the values published in [4] and with the theoretical model introduced in details in Sec. IV. The cross sections σ^{q+} decrease for higher fullerene charge states at a given projectile energy, and all cross sections decrease with increasing projectile energy.

The most detailed information about the postionization development of the fullerene ions is contained in the relative distributions of the fullerene fragment masses that we ob-

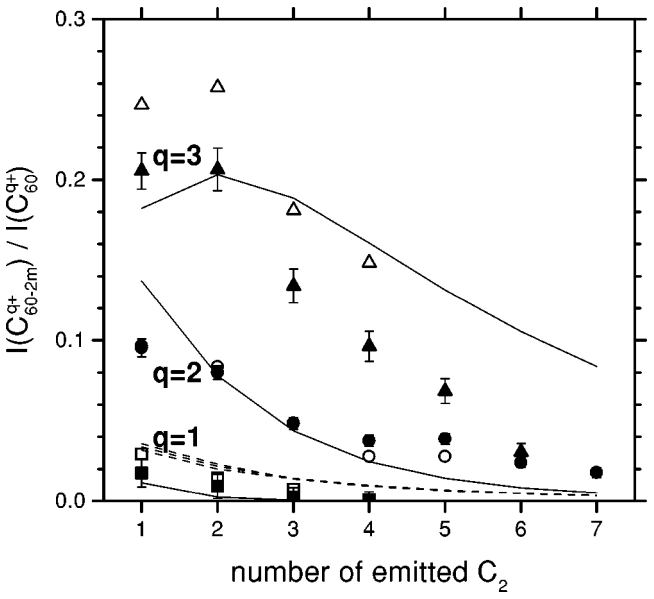

FIG. 4. The relative yield of the daughter fullerene ions $r_m^{q+} = I(C_{60-2m}^{q+})/I(C_{60}^{q+})$ with charge states $q=1$ up to 3 after 300-keV $H^+ + C_{60}$ collisions as a function of m, the number of emitted C_2 fragments. Error bars reflect only statistical errors. Hollow symbols represent values from Ref. [4]. The lines show the results of our calculations with (solid lines) and without (dashed lines) the delayed electron emission (see Sec. IV for more details).

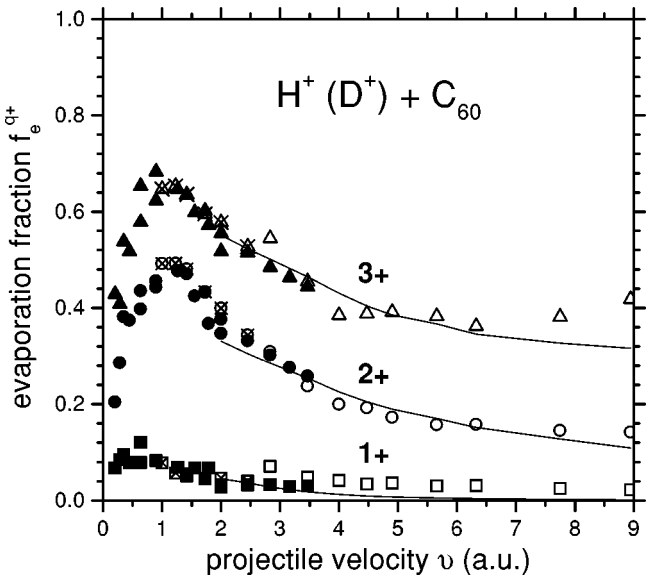

FIG. 5. Evaporation fractions f_e^{q+} for charge states $q=1$ (squares), $q=2$ (circles), and $q=3$ (triangles) as a function of the projectile velocity. Solid symbols represents our measurements for protons, partly already published in Ref. [6]; hollow symbols are the results taken from Ref. [4]. Crossed symbols show our results for $D^+ + C_{60}$ collisions. The curves show the results of our model calculations (see Sec. IV for more details).

tained at each projectile energy. As an example, Fig. 4 shows the distribution of fullerene ions after impact of 300-keV H^+. The intensity of the fragment fullerenes C_{60-2m}^{q+}, compared to the intensity of the C_{60}^{q+} ions with the same charge state q, decreases with increasing m, in agreement with the generally assumed successive C_2 evaporation picture. There are some exceptions, e.g., C_{50}^{2+} and C_{56}^{3+}, which may be an indication of a special stability of these fullerene types. Our data are compared with those from Ref. [4]. The general behavior of the distributions is similar.

The dependence of the evaporation fraction f_e^{q+} [see Eq. (2)] on the projectile velocity v is shown in Fig. 5. It has been used to reveal information about the excitation mechanism of C_{60}. In case of collisions of $He^{+,2+}$ with C_{60} this fraction decreases with an increasing projectile velocity proportional to $1/v$ (at least for $v \leqslant 1$ a.u.). Therefore it was concluded that the evaporation process is connected with ''nuclear energy loss'' [7,8]. Contrary, in the case of $H^+ + C_{60}$ collisions, the evaporation processes seem to be connected with the electronic excitation [6]: the fractions first increase with increasing proton velocity, reach a maximum at $v \sim 1-2$ a.u. and then slightly decrease again. The new data confirm our previous observations (Fig. 5). As expected, the observed fragment-ion distributions are identical for collisions of C_{60} with deuterium ions and with protons at the same projectile velocity. Moreover, the general tendency is confirmed by the experimental data taken from Ref. [4] which join quite well with our data. In addition, Fig. 5 shows a second nontrivial feature of the evaporation process: for each impact velocity, the evaporation fractions f_e^{q+} strongly increase with increasing charge state q from 1 to 3. This has already been seen in our previous work [6] but until now there has been no explanation of this phenomenon.

The two characteristic features of the distribution of fullerene ions, the increase of the ''daughter'' C_{60-2m}^{q+} ion intensity with increasing charge state q and the decrease with increasing number m of evaporated C_2 units, observed here in collisions with fast H^+ projectiles will be treated by a theoretical approach presented in the next section.

III. THEORETICAL MODEL

A. Basic concepts

A generally accepted physical picture of the process of ionization and fragmentation of fullerenes by fast-ion impact is based on characteristic time estimates. The collision time for protons in the considered energy interval (100 keV–10 MeV) is 10^{-16}–10^{-17} s. It is much shorter than the typical time of any rovibrational motion in the molecule which is about 10^{-13} s or longer. Therefore to a good approximation one can assume that the proton collides with a fixed in space ''frozen'' molecule and transfers to it some energy, without influencing the further development of the process. The energy is mainly transferred to electronic degrees of freedom since the cross section for elastic collision with nuclei is negligibly small for the considered energies. The deposited energy is partly spent for ionization (binding energy of electrons and their kinetic energy). However, some part of the deposited ''electronic'' energy is transferred to the vibrational degrees of freedom i.e., to the internal energy of the molecular ion. The subsequent dissociation of the ''hot'' molecular ion or ''evaporation'' of small fragments are much slower processes that may take from several picoseconds up

to several microseconds or possibly even longer. The cooling of the hot molecular ion also includes emission of photons and delayed electrons. Since the observation time in a usual TOF mass-spectroscopic experiment is about 1 μs the detected particles are created in both the ''fast'' excitation-ionization stage of the process as well as the ''slow'' relaxation stage.

Due to the complexity of the problem, to the best of our knowledge there is no theoretical description of the whole process of multiple ionization and fragmentation of fullerenes by ion impact. However, there were several attempts to describe theoretically or to model some parts of the process. A first estimate of the energy transfer in the fast-ion–fullerene collision has been made by LeBrun *et al.* [12] and Cheng *et al.* [14] on the basis of the plasmon excitation model. This model has also been used by Tsuchida *et al.* [4] for a description of proton-C_{60} collisions. Later it was suggested to estimate the deposited energy using the semiempirical formulas for electronic stopping cross sections for ions, considering C_{60} as a thin carbon film of corresponding density [5,10,11]. For lower velocities ($v \sim 1$) the energy deposition was calculated with the help of usual approaches in a stopping-power theory such as the electron-gas model [7,8] and the Firsov model [6].

The model for multiple ionization of fullerenes by ion impact has been suggested by Wohrer *et al.* [23]. The C_{60} molecule has been considered as composed of 60 independent carbon atoms whose positions are fixed during the collision time. The probability of *n*-fold ionization of the fullerene is expressed in terms of the ionization probability of an individual atom for a given impact parameter. For a practical application of the model the impact-parameter dependence of the ionization probability for the atom should be known. Another approach, restricted to single- and double-ionization only, has been used in [4,12,14], suggesting that the ionization probability is proportional to the probability of plasmon excitation.

The multifragmentation of C_{60} was modeled for the case of collisions with high-energy Xe ions [12,14] within the simple bond-breaking model. We do not know of any attempt to theoretically describe the production of daughter fullerenes C_{60-2m}^{q+} in fast-ion-C_{60} collisions. However, in slow-collision theory several models were used based on various types of statistical approaches, such as an evaporative ensemble model [24–26], the Rice-Ramsperger-Kassel-Marcus (RRKM) theory [27], or a model based on the maximum entropy principle [28]. The RRKM theory was used also for a description of C_{60} fragmentation by fast-proton impact [6], but only in order to estimate the internal energy from the experimental spectrum of the fragments.

Below we describe a model that combines the description of proton-impact-induced multiple ionization and the subsequent evaporation of C_2 fragments. Our main assumption is that the ionization-fragmentation process can be divided into three independent steps. The first step is the energy transfer from the fast projectile to the electronic system of the fullerene. Here the local electron-gas approximation by Lindhard and Scharff [29] is used for calculating the impact-parameter dependence of the mean energy loss and straggling in the proton-C_{60} collision.

The second step is electron emission (prompt electrons). Its separation as an independent step is justified by the fact that on the average the escape time of an ionized electron is about $10^{-14}-10^{-15}$ s which is much longer than the collision time but is still much shorter than any vibrational period. The lifetime of a typical autoionizing state is of the same order of magnitude. Therefore, we can assume that electron emission occurs when the scattered proton is already far away, but the target fullerene is still frozen. For a description of ionization we use the statistical energy deposition (SED) model by Russek-Meli [30] and Cocke [31] which we have recently further improved [32] and generalized for ion-molecule collisions [33].

The last step is quasiequilibrium evaporation of the neutral C_2 fragments. We suppose also that at this stage the delayed electron emission (quasithermoemission) is possible. To obtain the final distribution of daughter fullerenes we solve the differential rate equations that describe the evolution of the charge and mass state distributions during the detection time. The described model is semiempirical since it contains several free parameters that are fitted to obtained good agreement with the experiment. Details of the model are described below.

B. Energy deposition. Stopping power and straggling

In order to calculate the deposited energy we use the approximation well known in the stopping power theory, the so-called local-plasma or local- (electronic) density approximation (LDA). It is based on the idea of Lindhard and Scharff [29], who suggested considering each volume element of the target atom independently as an electron gas of uniform density that is equal to the electron density of the atom. Using the known stopping power of an electron gas and integrating over the target volume with the known electron density, a good description of the energy loss in atomic and molecular targets is achieved [34–36]. We use this approximation in order to calculate the energy deposition in an ion-fullerene collision.

We assume that the projectile ion is a point charge Z_1 moving along a straight-line trajectory with a constant velocity v and an impact parameter $\mathbf{b}$ which is measured from the center of mass of the target C_{60} molecule. The energy loss in a collision is a statistical process and the transferred energy may be characterized by the mean energy and energy straggling. Within the LDA the mean deposited energy for a certain ion trajectory can be calculated as a line integral along the trajectory:

$$\bar{E}_d(\mathbf{b}) = \frac{4\pi Z_1^2}{v^2} \int_{-\infty}^{\infty} dz\, \rho(\mathbf{r}) L(\rho(\mathbf{r}), v), \tag{3}$$

where the z axis is chosen along the ion-beam direction, $\mathbf{r} = \{\mathbf{b}, z\}$, $\rho(\mathbf{r})$ is the electron density of the fullerene, and $L(\rho(\mathbf{r}), v)$ is the usual stopping number. Similarly, the energy straggling as function of the impact parameter may be

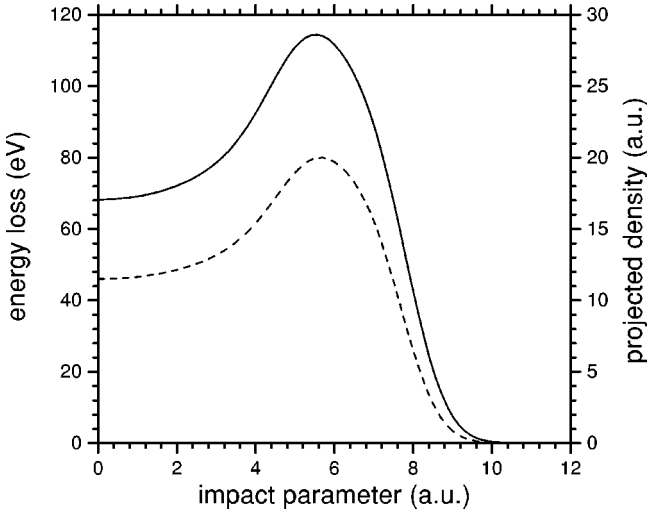

FIG. 6. Projected electron density in the C_{60} target (dashed line and right axis) and mean energy loss calculated for 300-keV protons (solid line and left axis) as a function of the impact parameter.

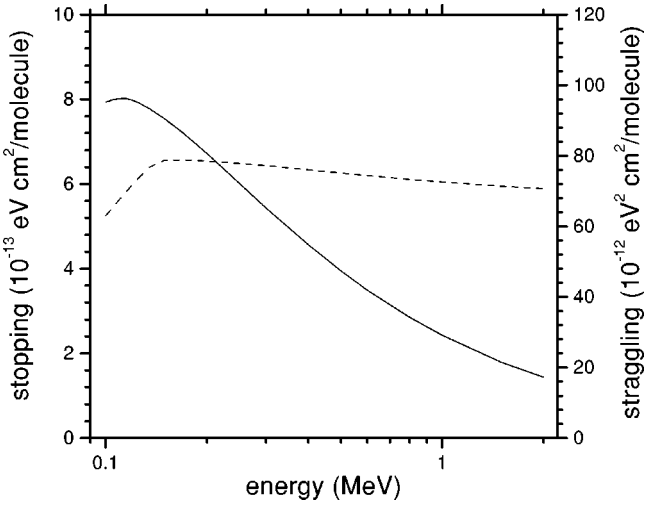

FIG. 7. Stopping power of C_{60} for protons (solid line and left axis) and straggling (dashed line and right axis) as a function of the proton energy, calculated within the Lindhard-Scharff model.

calculated (see Ref. [32] for further details). Integration over impact parameters gives the stopping cross section and total straggling.

The distribution of electronic density in the C_{60} molecule has been taken from Puska-Nieminen calculations [37] within the modified jellium model. As an example, Fig. 6 shows the impact-parameter dependence of the mean energy loss calculated according to Eq. (3) for the proton energy of 300 keV. In the same figure the projected electron density of the fullerene (integrated along z) is presented. One notes that both curves are similar showing a characteristic behavior [6,8] with a maximum at about 6 a.u. which is close to the average position of the nuclear cage. The energy loss is varying from $\sim$70 eV for the trajectory passing through the center of the fullerene to $\sim$120 eV at the maximum. Similar distributions have been calculated for other energies. The calculated total-energy-loss cross section and straggling as function of the proton energy are shown in Fig. 7. Comparing the results with the energy loss of a proton to carbon atoms [38] we note that the electronic energy loss is approximately 2–7 % less than predicted by Bragg's rule which states that the stopping power of a molecule is equal to the sum of the stopping power of its constituent atoms. Unfortunately, to the best of our knowledge, there are no experimental data for the stopping power of gaseous C_{60} for protons. Our calculations are close to that calculated in [39] for crystalline C_{60}.

C. Multiple ionization

The cross section for multiple ionization of C_{60} has been calculated using the extended version of the Russek-Meli-Cocke SED model [32,33]. Within this model the cross section is proportional to the volume of phase space available in each ionization state, and it is directly related to the deposited energy and the ionization potentials of the various levels. As was shown in [30] the probability of n-fold ionization for a certain deposited energy E_d can be expressed as

$$P_n(E_d)=\frac{\binom{N_e}{n} g^n S_n(E_k/\mathcal{E}_1)}{\sum_{i=1}^{N_e}\binom{N_e}{i} g^i S_i(E_k/\mathcal{E}_1)}. \tag{4}$$

Here N_e is the number of considered electrons, $\binom{N_e}{n}$ is the binomial coefficient, and E_k is the kinetic energy available to the electrons if the residual ion is left in the nth ionization state. The relation between the deposited energy and the kinetic energy E_k carried off by the ionized electrons is given by

$$E_k=E_T-\sum_{i=1}^{n}\mathcal{E}_i-E_R(n), \tag{5}$$

where $\mathcal{E}_i$ is the ith ionization energy and $E_R(n)$ is the residual excitation of the remaining ion. The latter consists of the energy transferred to the vibrational degrees of freedom (ΔE_{in}) but can also contain some residual electronic excitations. The dimensionless parameter g is proportional to the mean square matrix element of a single ionization and it is supposed that for multiple ionization the mean square matrix element behaves according to a power law. The constant g is considered as a free parameter, its value being fitted to give a good agreement with the experimental cross-section ratios. For the factor $S_n(E_k/\mathcal{E}_i)$ characterizing the density of the final states a simple expression was obtained [30] (see Ref. [32] for details).

Given the mean deposited energy and straggling for a certain impact parameter, the probability of multiple ionization can be obtained by a convolution of the probability (4) with the deposited energy distribution,

$$P_n(\mathbf{b})=\int dE_d' P_n(E_d') w(E_d',\mathbf{b}). \tag{6}$$

For the $w(E_d',\mathbf{b})$ distribution we have used the power form suggested in Ref. [32]. Then the total cross section of multiple ionization is

$$\sigma_n = \int d^2\mathbf{b}\, P_n(\mathbf{b}). \tag{7}$$

Using Eqs. (4)–(7) we have calculated the total multiple-ionization cross sections for a range of proton energies from 100 keV to 2 MeV. The results are presented in Fig. 3, where they are compared with the experimental results of this work and [4]. We show the results for three different values of the g factor to demonstrate the sensitivity of the results to variations of g. It is clear that by fitting the free parameter g it is possible to describe rather accurately the multiple-ionization cross sections for $q>1$. Single ionization is overestimated by the model (see the discussion in Sec. IV). We note, however, that the calculated cross sections describe emission of only prompt electrons. The delayed electron emission can modify the final charge distribution of fullerenes measured in experiment. This effect is considered in the next section.

D. Evaporation of C_2 fragments and delayed electron emission

In the first two stages of the collision the hot fullerene ions C_{60}^{q+} are produced. Since part of the deposited energy is transferred to the internal energy, the fullerene ions are vibrationally excited. Furthermore, they may be electronically excited. The hot fullerene ions may then emit C_2 neutral fragments and delayed electrons. The cooling process includes also fluorescence [40,41] but in the first approximation we ignore it and consider only two processes of cooling: C_2 and electron emission. We assume that they may be considered as quasiequilibrium processes although the real equilibration is probably not achieved within the observation time (see the discussion below).

To characterize the distribution of fullerene ions over charge and mass we introduce the fractions F_m^q which give the relative population of the ion C_{60-2m}^{q+}. The time evolution of the fractions is described by a system of rate equations

$$\frac{dF_m^q(t)}{dt} = -F_m^q(t)(k_{m\to m+1}^q + k_m^{q\to q+1}) + F_m^{q-1}(t)k_m^{q-1\to q} + F_{m-1}^q(t)k_{m-1\to m}^q. \tag{8}$$

The rate constants $k_{m\to m+1}^q$ determine the C_2 evaporation rates while $k_m^{q\to q+1}$ determine the delayed ionization rates. The first term in Eq. (8) describes a decrease of the fraction F_m^q due to emission of the C_2 fragments and delayed electrons, the second and third terms describe an increase of the fraction due to C_2 emission from the previous even-mass fullerene of the same charge and due to electron emission from the fullerene of the same mass but lower charge, respectively. At the initial moment only fractions F_0^q corresponding to C_{60}^{q+} ions are non-zero;[2] they are supposed to be proportional to the ionization cross sections calculated in Sec. III C. The solution of the rate equations at the final moment of observation $t_{max}=1$ μs characterizes the final charge and mass distribution of the fragments.

The key problem is the evaluation of the rate constants. We have chosen the Arrhenius-type representation which is often used in practical calculations [25,40,42,43]:

$$k_{m\to m+1}^q = A_{ev}\exp(-E_a/k_BT), \tag{9}$$

$$k_m^{q\to q+1} = A_{ion}\exp(-\mathcal{E}_{q+1}/k_BT). \tag{10}$$

Here k_B is the Boltzmann constant, T is the temperature describing the internal energy of the fullerene ion, E_a is the activation energy (threshold) of C_2 evaporation, $\mathcal{E}_{q+1}$ is the $(q+1)$th ionization threshold. In the literature there is a big discussion about the value of the activation energy of C_2 evaporation and the value of the preexponential factor A_{ev} that varies by many orders of magnitude in different papers (see, for example, [44]). The latest experimental and theoretical papers favor a high value of the activation energy $E_a = 10-12$ eV [45,46] as well as high values of $A_{ev}\sim 10^{19}-10^{21}$ s^{-1} [44,47]. The ionization thresholds for fullerene ions are better established. We have taken the values from Refs. [49,50]: $\mathcal{E}_2=11.4$ eV, the electron binding energy in C_{60}^+; $\mathcal{E}_3=16.6$ eV (C_{60}^{2+}); and $\mathcal{E}_4=20$ eV (C_{60}^{3+}). As follows from experimental data, the activation energy E_a does not depend significantly on the charge state of the ion and on the number of evaporated C_2 dimers [47]. Similarly the ionization thresholds are practically independent of the fragment mass [49]. There is a big variation also in the preexponential factor for the delayed electron emission A_{ion} derived from experiments or from theoretical considerations. The values vary from 10^{13} s^{-1} [42] to 10^{17} s^{-1} [51]. We have chosen the value 2×10^{16} s^{-1} as suggested by Klots [48] and used in model calculations [40]. The temperature T in Eqs. (9) and (10) is connected with the internal energy by the equation [25]

$$E_{in} = \frac{(3\tilde{n}-6)h\nu}{\exp[h\nu/k_BT]-1}, \tag{11}$$

where $\tilde{n}=60-2m$ is the number of atoms in the fullerene, and the average vibrational frequency for ions was chosen the same as for neutral fullerene $\nu=2.7\times10^{13}$ Hz, taken from [52]. At each act of evaporation the internal energy is diminished by the value $E_a+E_{kin}+E_{C_2}$, where the evaporated fragment kinetic energy E_{kin} and internal energy E_{C_2} were approximated by $2k_BT$ [25]. At each act of the delayed electron emission the internal energy is diminished by

[2] In the calculations we ignore neutral excited C_{60}. Since the first ionization threshold is comparatively small (7.54 eV) all hot neutrals quickly ionize to C_{60}^+. Those fullerenes that remain neutral should not be considered since they are not registered in the experiment.

$\approx \mathcal{E}_{q+1}$. Since the temperature of the target gas was about 550 °C, the initial internal energy was about 5 eV. After the collision the internal energy is increased by ΔE_{in}. We suppose that the energy transferred to the vibrational degrees of freedom during the collision is proportional to the average deposited energy $\langle E_d \rangle$

$$\Delta E_{in} = \alpha \langle E_d \rangle, \tag{12}$$

where α is a parameter (which is about 0.2, see Sec. IV). For simplicity we suppose that the spectrum of the transferred internal energy is described by the same form as the total deposited energy with parameters fitted to the average transferred internal energy and its straggling; similarly, the latter is assumed to be proportional to the average straggling of the deposited energy $\Omega_{in}^2 = \alpha^2 \langle \Omega^2 \rangle$. From our calculations of the deposited energy it follows that the average deposited energy is varying from 156 eV for 100 keV protons to 28 eV for 2 MeV protons, while the average straggling is varying only slightly from 111 to 118 eV in this energy range.

The calculation procedure was the following. For each of the transferred internal energy the system of the rate equations (8) with the corresponding rate constants (9) and (10) was solved up to $t = 1$ μs. The final charge and mass distribution was averaged over the transferred internal energy spectrum. The results of the calculations are discussed in the following section.

IV. COMPARISON OF THE EXPERIMENTAL RESULTS WITH THE MODEL CALCULATIONS AND DISCUSSION

First we discuss the multiple-ionization cross sections (the yields of fullerenes of different charge). The calculated cross sections for production of fullerenes of different charge are compared with the experimental results in Fig. 8. The dashed curves give the results of the calculations within the SED model with the parameter $g = 0.007$. We note that this value is very close to that obtained earlier for the ion-atom [32] and ion-molecule [33] collisions. The solid curves show the cross sections corrected for the emission of the delayed electrons. We see that the cross sections for the $2^+ - 4^+$ ionization fit the experimental data quite well. The calculated single ionization cross section overestimates the experiment by a factor of 2. We think that such a discrepancy is within the accuracy of the model and possibly also of the experiment. Due to its statistical nature the model can hardly be more accurate for the single ionization. We note also that at this stage of the discussion, when only the cross sections for ionization are considered, it is not necessary to introduce the corrections due to delayed electron emission. The same quality of agreement can be obtained also without corrections by slightly increasing the g parameter (compare with Fig. 3).

We next discuss the predictions of the C_2 evaporation model. As an example, we show in Fig. 4 the charge and mass distribution of daughter fullerenes calculated for a proton energy of 300 keV. The dashed curves show the results of calculation of the relative yield r_m^{q+} disregarding the delayed electron emission. The parameters of the evaporation rate

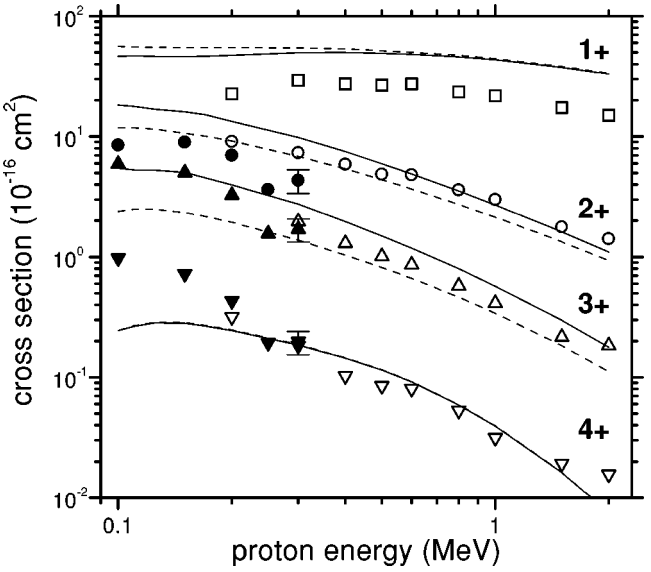

FIG. 8. Cross sections of fullerene ion production σ^{q+} for different proton energies. Experimental data are the same as in Fig. 3. Dashed lines show the results of calculations within the SED model (only prompt electron emission). Solid lines include corrections due to the C_2 evaporation and the delayed electron emission.

constant were chosen to be $A_{ev} = 2 \times 10^{19}$ s^{-1}, $E_a = 11.6$ eV, and $\alpha = 0.23$. The calculated ratios are practically identical for different charge states. The results clearly disagree with the experiment which shows much larger evaporation fractions for higher charge states. Very similar model results are obtained with account for the delayed electron emission with $A_{ion} = 2 \times 10^{16}$ s^{-1} and experimental values of ionization thresholds. The situation can only be improved by increasing the contribution of the delayed electron emission. We prefer not to increase the preexponential factor in order to preserve the difference of several orders of magnitude in A_{ev} and A_{ion} as follows from the experiment [53]. Instead we diminish the threshold values. The solid curves in Fig. 4 show the distributions calculated with $\mathcal{E}_2 = 8.9$ eV, $\mathcal{E}_3 = 9.6$ eV and $\mathcal{E}_4 = 14$ eV. Now the calculated distributions generally correspond to the experiment. The physical explanation of the smaller threshold energies lies in the residual electronic excitations of the fullerene after the collision at least until the first C_2 emission; actually it is very probable that the ionization is accompanied by electronic excitations. Some of the excited states may be sufficiently long living. This question has already been discussed for neutral fullerenes in connection with the nature of the delayed electron emission [54–57]. It was suggested that, at least partly, the delayed electron emission is associated with autoionization of the metastable triplet excited states [54] or highly excited autoionizing states [58]. We think it is plausible to assume the existence of some long-living excited states also for fullerene ions. Effectively their excitation would lead to the decrease of the ionization thresholds.

In Fig. 5 the calculated and measured evaporation fractions are compared. One can see that the chosen set of parameters permits us to describe the experimental data quite well. Concluding the comparison of the model calculations

with the experiment we note that in spite of considerable uncertainty in the model parameters, especially in the part describing the C_2 evaporation and delayed electron emission rates, the fitting procedure indicates some basic physical features which are almost independent of the particular choice of parameters. It seems that the delayed electron emission is an important factor determining the final charge and mass distribution of fullerenes in TOF experiments. If it is so, then the residual excitation of fullerenes may play a crucial role in explaining the experimental data. In the described model we supposed that the energy transferred to the vibrational degrees of freedom is proportional to the total deposited energy and does not depend on the charge state of the ion fullerene. There may be arguments claiming that higher degrees of ionization are associated with higher temperature. We plan to explore this possibility in future work.

V. CONCLUSIONS

We have presented the results of our time-of-flight measurements of the yields of all charged fragments produced in ionization and fragmentation of C_{60} by proton and deuteron impact in the collision energy range of 50–300 keV. Our results are in a good agreement with the published data at lower and higher energies. The measured charge and mass distributions are formed by a fast process of primary collision and prompt electron emission as well as by a comparatively slow process of C_2 evaporation and delayed electron emission from the hot fullerene ion. We suggested a model that describes both the fast and the slow stages of the process. The model is semiphenomenological in the sense that it contains adjustable parameters. In spite of this, analyzing the experimental data within the framework of the model we are able to draw some conclusions about the nature of the complicated process of C_{60} fragmentation. It is clear that the successive evaporation of C_2 neutral dimers can explain the mass distribution of the fullerene fragments. However, to describe the charge distributions it is apparently necessary to take into account the delayed electron emission, too. We also have an indication that the latter process occurs in the excited fullerene ion. Therefore, the cooling of the hot fullerene is not an equilibrium process. The equilibration between electronic and vibrational degrees of freedom is not yet achieved when the fullerene emits delayed electrons and C_2 fragments. This is consistent with other observations discussed recently in review papers by Campbell and Levine [59,60].

ACKNOWLEDGMENTS

We are indebted to R. Schmidt for stimulating discussions. N.M.K. is grateful to the Bielefeld University for hospitality. This work was supported in part by the Deutsche Forschungsgemeinschaft (DFG) in the project ''Stralungswechselwirkungen'' and has been carried out within the framework of the European network LEIF (No. HRPI-CT-1999-40012).

[1] D.C. Lorents, Comments At. Mol. Phys. **33**, 125 (1997).
[2] E.E.B. Campbell and F. Rohmund, Rep. Prog. Phys. **63**, 1061 (2000).
[3] A. Reinköster, U. Werner, and H.O. Lutz, Europhys. Lett. **43**, 653 (1998); U. Werner, V.N. Kondratyev, and H.O. Lutz, Nuovo Cimento A **110**, 1215 (1997).
[4] H. Tsuchida, A. Itoh, Y. Nakai, K. Miyabe, and N. Imanishi, J. Phys. B **31**, 5383 (1998).
[5] H. Tsuchida, A. Itoh, K. Miyabe, Y. Bitoh, and N. Imanishi, J. Phys. B **32**, 5289 (1999).
[6] J. Opitz, H. Lebius, S. Tomita, B.A. Huber, P. Moretto Capelle, D. Bordenave Montesquieu, A. Bordenave Montesquieu, A. Reinköster, U. Werner, H.O. Lutz, A. Niehaus, H.T. Schmidt, and H. Cederquist, Phys. Rev. A **62**, 022705 (2000).
[7] T. Schlathölter, O. Hadjar, R. Hoekstra, and R. Morgenstern, Phys. Rev. Lett. **82**, 73 (1999).
[8] T. Schlathölter, O. Hadjar, J. Manske, R. Hoekstra, and R. Morgenstern, Int. J. Mass Spectrom. **192**, 245 (1999).
[9] Y. Nakai, A. Itoh, T. Kambara, Y. Bitoh, and Y. Awaya, J. Phys. B **30**, 3049 (1997).
[10] A. Itoh, H. Tsuchida, T. Majima, and N. Imanishi, Phys. Rev. A **59**, 4428 (1999).
[11] A. Itoh, H. Tsuchida, T. Majima, S. Anada, A. Yogo, and N. Imanishi, Phys. Rev. A **61**, 012702 (1999).
[12] T. LeBrun, H.G. Berry, S. Cheng, R.W. Dunford, H. Esbensen, D.S. Gemmell, E.P. Kanter, and W. Bauer, Phys. Rev. Lett. **72**, 3965 (1994); Nucl. Instrum. Methods Phys. Res. B **98**, 479 (1995).
[13] R. Ali, H.G. Berry, S. Cheng, R.W. Dunford, H. Esbensen, D.S. Gemmell, E.P. Kanter, T. LeBrun, L. Young, and W. Bauer, Nucl. Instrum. Methods Phys. Res. B **98**, 545 (1995).
[14] S. Cheng, H.G. Berry, R.W. Dunford, H. Esbensen, D.S. Gemmell, E.P. Kanter, T. LeBrun, and W. Bauer, Phys. Rev. A **54**, 3182 (1996).
[15] J. Becker, K. Beckord, U. Werner, and H.O. Lutz, Nucl. Instrum. Methods Phys. Res. A **337**, 409 (1994).
[16] U. Werner, J. Becker, K. Beckord, and H.O. Lutz, Nucl. Instrum. Methods Phys. Res. B **123**, 298 (1997).
[17] B. Siegmann, U. Werner, and H.O. Lutz, Aust. J. Phys. **52**, 545 (1999).
[18] A. Reinköster *et al.* (unpublished).
[19] M.O. Larsson, P. Hvelplund, M.C. Larsen, H. Shen, H. Cederquist, and H.T. Schmidt, Int. J. Mass Spectrom. **177**, 51 (1998).
[20] T. Schlathölter, R. Hoekstra, and R. Morgenstern, J. Phys. B **31**, 1321 (1998).
[21] J. Abrefah, D.R. Olander, M. Balooch, and W.J. Siekhaus, Appl. Phys. Lett. **60**, 1313 (1992).
[22] B. Walch, C.L. Cocke, R. Voelpel, and E. Salzborn, Phys. Rev. Lett. **72**, 1439 (1994).
[23] K. Wohrer, M. Chabot, A. Touati, and R.L. Watson, Nucl. Instrum. Methods Phys. Res. B **88**, 174 (1994).
[24] C.E. Klots, Z. Phys. D: At., Mol. Clusters **21**, 335 (1991).

[25] F. Rohmund, A.V. Glotov, K. Hansen, and E.E.B. Campbell, J. Phys. B **29**, 5143 (1996).
[26] R. Vandenbosch, Phys. Rev. A **59**, 3584 (1999).
[27] R. Ehlich, M. Westerburg, and E.E.B. Campbell, J. Chem. Phys. **104**, 1900 (1996).
[28] E.E.B. Campbell, T. Raz, and R.D. Levine, Chem. Phys. Lett. **253**, 261 (1996).
[29] J. Lindhard and M. Scharff, Mat. Fys. Medd. K. Dan. Vidensk. Selsk. **27**, (15), 1 (1953).
[30] A. Russek and J. Meli, Physica (Utrecht) **46**, 222 (1970).
[31] C.L. Cocke, Phys. Rev. A **20**, 749 (1979).
[32] N.M. Kabachnik, V.N. Kondratyev, Z. Roller-Lutz, and H.O. Lutz, Phys. Rev. A **56**, 2848 (1997).
[33] N.M. Kabachnik, V.N. Kondratyev, Z. Roller-Lutz, and H.O. Lutz, Phys. Rev. A **57**, 990 (1998).
[34] E. Bonderup, Mat. Fys. Medd. K. Dan. Vidensk. Selsk. **35**, (17), 1 (1967).
[35] C.C. Rousseau, W.K. Chu, and D. Powers, Phys. Rev. A **4**, 1066 (1971).
[36] Y.J. Xu, G.S. Khandelwal, and J.W. Wilson, Phys. Rev. A **29**, 3419 (1984).
[37] M.J. Puska and R.M. Nieminen, Phys. Rev. A **47**, 1181 (1993).
[38] H.H. Andersen and J.F. Ziegler, *Hydrogen Stopping Powers and Ranges in All Elements* (Pergamon, New York, 1977).
[39] I. Abril, R. Garcia-Molina, and N.R. Arista, Nucl. Instrum. Methods Phys. Res. B **90**, 72 (1994).
[40] R. Mitzner and E.E.B. Campbell, J. Chem. Phys. **103**, 2445 (1995).
[41] K. Hansen and E.E.B. Campbell, J. Chem. Phys. **104**, 5012 (1996).
[42] C.E. Klots, Z. Phys. D: At., Mol. Clusters **20**, 105 (1991).
[43] M. Foltin, M. Lezius, P. Scheier, and T.D. Märk, J. Chem. Phys. **98**, 9624 (1993).
[44] C. Lifshitz, Int. J. Mass Spectrom. **198**, 1 (2000).
[45] A.D. Boese and G.E. Scuseria, Chem. Phys. Lett. **294**, 233 (1998).
[46] J. Laskin, B. Hadas, T.D. Märk, and C. Lifshitz, Int. J. Mass Spectrom. **177**, L9 (1998).
[47] S. Matt, O. Echt, M. Sonderegger, R. David, P. Scheier, J. Laskin, and T.D. Märk, Chem. Phys. Lett. **303**, 379 (1999).
[48] C.E. Klots, Chem. Phys. Lett. **186**, 73 (1991).
[49] R. Wörgötter, B. Dünser, P. Scheier, and T.D. Märk, J. Chem. Phys. **101**, 8674 (1994).
[50] H. Steger, J. Holzapfel, A. Hielscher, W. Kamke, and I.V. Hertel, Chem. Phys. Lett. **234**, 455 (1995).
[51] A. Bekkerman, B. Tsipinyuk, A. Budrevich, and E. Kolodney, J. Chem. Phys. **108**, 5165 (1998).
[52] R.E. Stanton and M.D. Newton, J. Phys. Chem. **92**, 2141 (1988).
[53] K. Hansen and O. Echt, Phys. Rev. Lett. **78**, 2337 (1997).
[54] Y. Zhang and M. Stuke, Phys. Rev. Lett. **70**, 3231 (1993).
[55] K.R. Lykke, Phys. Rev. Lett. **75**, 1234 (1995).
[56] M. Stuke and Y. Zhang, Phys. Rev. Lett. **75**, 1235 (1995).
[57] C.E. Klots and R.N. Compton, Phys. Rev. Lett. **76**, 4092 (1996).
[58] A.A. Vostrikov, D.Yu. Dubov, and A.A. Agarkov, Tech. Phys. Lett. **21**, 715 (1995).
[59] E.E.B. Campbell and R.D. Levine, Comments At. Mol. Phys. Comments on Mod. Phys. D **1**, 155 (1999).
[60] E.E.B. Campbell and R.D. Levine, Annu. Rev. Phys. Chem. **51**, 65 (2000).